Applied Animal Behaviour Science 287 (2025) 106636

Contents lists available at ScienceDirect

Applied Animal Behaviour Science

journal homepage: www.elsevier.com/locate/applanim

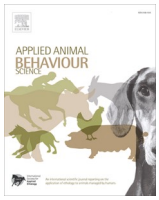

Monitoring shrimp behavior in relation to feed provision, location and time of day in an experimental aquaculture pond

Jean-Benoît Darodes de Tailly [a], Ignacio Martinez Alpiste [b], Matthew A.G. Owen [c,1], Jonas Keitel [c], Jose M. Alcaraz-Calero [b], Katherine A. Sloman [a,*], Mhairi E. Alexander [a]

[a] Institute of Biomedical and Environmental Health Research, School of Health & Life Sciences, University of the West of Scotland, Lanarkshire G72 0LH, United Kingdom
[b] School of Computing, Engineering & Physical Sciences, University of the West of Scotland, Paisley PA1 2BE, United Kingdom
[c] Skretting Aquaculture Innovation (AI), Stavanger 4016, Norway

ARTICLE INFO

Key words:
Feeding behavior
Penaeid shrimp
Shrimp pond
Tracking software
YOLACT

ABSTRACT

A primary challenge in penaeid shrimp farming is suboptimal feed utilization, leading to inefficiencies in production. Better insights into shrimp feeding behavior may provide pathways to address these inefficiencies. While previous studies have highlighted the influence of feed dispersal and time of day on penaeid shrimp behavior in controlled settings, comprehensive analyses of their behavior in production ponds remain limited. The aim of this study was to understand shrimp group feeding behavior in ponds, and how this relates to feed provision, location within the pond, and time of day. Three consecutive trials were performed in an experimental aquaculture pond (28 m^2) in Zhuhai, China, stocked with juvenile whiteleg shrimp *Litopenaeus vannamei* (7.1 ± 0.4 g, mean ± S.E.) at 20 $ind.m^{-2}$. Each trial comprised 7 days of acclimation followed by 6 days of observation. Three underwater cameras were placed on the bottom of the pond at different locations, with feed provided at different pond locations six times a day between 07:00 and 19:00. Shrimp within the field of view for each camera were tracked using a combination of automated (YOLACT, You Only Look At CoefficienTs) and manual techniques, allowing for calculation of key behavioral metrics associated with individual and group behavior. Shrimp gathered in large numbers around the feeding area shortly after feed provision (i.e. 1 min after) and a gradient in shrimp density was found 10 min after feed provision from high densities inside the feeding area (89.8 ± 5.5 $ind.m^{-2}$) to low densities on the opposite edge of the pond (11.9 ± 2.3 $ind.m^{-2}$). Shrimp were more evenly distributed across the pond at night compared to daytime. Although no schooling behavior was observed, shrimp movements were on average twice as fast across the whole pond shortly after feed provision compared to before feeding. Movements inside the feeding area were less polarized (i.e. reduced alignment in the animals' heading direction relative to that of the group) after feed provision. This study provides a first insight into shrimp feeding behavior in aquaculture ponds, which could help with inefficiencies in production of this species.

1. Introduction

In shrimp aquaculture, feed can comprise up to half of total production costs (Silva et al., 2012; Engle et al., 2017). However, with little known about penaeid shrimp feeding behavior in large scale aquaculture ponds, key research questions remain, including how shrimp are distributed in ponds and how they react towards feeders during feeding (reviewed by Darodes de Tailly et al., 2021). Previous laboratory observations reported significant effects of feed dispersion and time of day on shrimp behavior. For example, *Litopenaeus vannamei* fed a commercial ration three or four times a day showed greater food ingestion between 12:00 and 14:00 compared to feeding seven times a day (De Lima et al., 1931), and substrate exploration in the search for food was most intense in *L. vannamei* 7 h after the start of the light phase (Pontes et al., 2006). Anecdotal observations from scuba dives in large Ecuadorian shrimp ponds reported large scale changes in behavior in response to feed provision and the potential for shrimp to form large swarms (or troops) (McNeil, 2001). However, observations on swarm shape, size

* Corresponding author.
E-mail address: Katherine.Sloman@uws.ac.uk (K.A. Sloman).
[1] Current address: WorldFish, Jalan Batu Maung, Batu Maung, Bayan Lepas, Penang 11960, Malaysia.

https://doi.org/10.1016/j.applanim.2025.106636
Received 5 May 2024; Received in revised form 4 April 2025; Accepted 15 April 2025
Available online 16 April 2025

distribution, movements and triggers of such formations have not been studied. In particular, how shrimp behave in unfed areas of ponds remains largely unknown.

Although many shrimp farms still rely on manual hand feeding, an increasing number use automated feeders where location of feeders and distribution of food can have implications for animal welfare. The bottom layer of ponds is susceptible to localized areas of hypoxia through accumulation of unconsumed feed and feces (Zhang et al., 2006) and high stocking densities can increase competition for access to feeding areas (Sanchez et al., 2005). Changing feeder location within the pond several times during the production cycle may potentially help alleviate such issues. This is well documented in finfish aquaculture where random distribution of feed across space and time allows more even access and prevents monopolization by dominant fish (Kadri et al., 1996). Observations in shrimp ponds in Ecuador reported that the largest individuals accessed feed first (McNeil, 2001); whether shrimp exhibit anticipatory behavior when feeders start spreading pellets as seen in finfish aquaculture (Martins et al., 2012) is unknown. Observing shrimp behavior under commercial conditions remains a challenge as they are prone to substantial water turbidity (Lai et al., 2022). Furthermore, penaeid shrimp are benthic feeders making assessment of feeding activity from the surface impossible. To date, evaluation of feed intake mostly relies on the observation of feeding trays after feed is provided, often resulting in inaccurate estimates of feed consumption and overfeeding (Smith and Tabrett, 2013; Ullman et al., 2017; Reis et al., 2020, 2022). New techniques for real-time monitoring of shrimp feeding behavior in ponds are required. Recent developments in passive acoustic monitoring (PAM) can provide an accurate proxy of shrimp feeding (Smith and Tabrett, 2013), and may be indicative of large-scale behaviors but do not capture the behavioral detail provided by visual observations.

Although largely dependent on underwater visibility, computer vision represents a valuable approach for monitoring shrimp behavior (Darodes de Tailly et al., 2021). Understanding shrimp feeding behaviour has traditionally relied on visual observation of feeding trays, which is difficult to achieve in a pond setting. Within controlled environments, the development of automated tracking software has reduced observer bias and allowed behavioural tracking over longer periods of time (Noldus et al., 2001). In finfish aquaculture, computer vision has proven efficient in obtaining key metrics related to school cohesion and activity (e.g. Xu et al., 2006; Sadoul et al., 2014; Zhou et al., 2017, 2018), which are particularly relevant for assessing fish appetite (Zhou et al., 2017, 2018) and welfare (Israeli and Kimmel, 1996; Xu et al., 2006; Sadoul et al., 2014; Pautsina et al., 2015). Traditionally, the use of computer vision in tracking aquatic animals relied on techniques such as image thresholding, based on the contrast between the observed animals (foreground) and the bottom of the observation arena (background) (Panadeiro et al., 2021). Such techniques are suitable in controlled environments such as indoor tanks (Yang et al., 2021), however pond conditions, especially in shrimp farming, represent a challenge in terms of contrast, visibility and illumination (Reis et al., 2022). Many of the issues associated with these tracking tools can be solved by applying deep learning-based object detection techniques (Martinez-Alpiste et al., 2024). These deep learning algorithms based on neural networks such as YOLO (You Only Look Once, Redmon et al., 2016) and YOLACT (You Only Look At CoefficienTs), represent alternatives to traditional detection methods and have recently been used for the automatic recognition and localization of aquatic animals in complex environments (e.g. Li et al., 2016; Pedersen et al., 2019; Cao et al., 2020; Mahmood et al., 2020; Lai et al., 2022). Deep learning algorithm methods have a good detection accuracy with potential application in an industry-context. The objective of the present study was to use computer vision techniques to provide an insight into shrimp feeding behavior in an experimental aquaculture pond. Specifically, the effects of three different parameters on shrimp behavior were assessed: (i) provision of feed, (ii) time of day, and (iii) displacement of the feeding area.

2. Materials and methods

2.1. Pond preparation and shrimp acclimation

For each experiment trial (n = 3), shrimp (*L. vannamei*, 7.1 ± 0.4 g, mean ± S.E) were stocked at a density of 20 individuals.m^{-2} in an experimental observation pond (7 ×4×0.5 m, length x width x water depth) at Skretting's research facilities in Zhuhai, China. The pond was lined with HDPE (High Density PolyEthylene) black plastic sheet. Feed (Shihai, Skretting China) was provided at a daily rate of 8 % of the estimated pond biomass in equal portions six times a day. Meals were provided at 7:30, 10:00, 12:00, 14:00, 16:00 and 19:00. At the onset of each trial, three 1 kg batches of shrimp were weighed to determine the shrimp count per kilogram. Pond biomass was estimated by employing standard growth curves provided by the feed manufacturer, taking into account 100 % survival rate over the short trial period. Water changes were performed with fresh water when turbidity was considered too high to allow visual observation of the animals (i.e. > 5 NTU, Nephelometric Turbidity Units), with a maximum of 15 % of the total volume of water being changed at any one time. 5 NTU was taken as the threshold for this study based on preliminary analysis of camera footage. Once stocked, shrimp were acclimated to the pond for 7 days before observations started.

During trials, water quality was monitored daily; pH was maintained at 8.2 ± 0.1 (mean ± S.E.), salinity at 4.3 ± 0.5 g.L^{-1}, and concentrations of ammonia and nitrite were kept below the safe limits provided by Lin and Chen (2001, 2003) (i.e. 0.3 ± 0.1 mg.L^{-1} and 0.1 ± 0.0 mg.L^{-1}, for Total Ammonia Nitrogen (TAN) and nitrites, respectively). Temperature was 31.1 ± 0.5 ºC (trial 1; mean ± S.E.), 30.2 ± 0.3 ºC (trial 2), 27.2 ± 0.7 ºC (trial 3). Dissolved oxygen was maintained above 5 mg.L^{-1} through the use of four airstones and an air pump. The observation pond was entirely covered with a semi-transparent tarpaulin, allowing for better control of oxygen and pH parameters while avoiding the occurrence of phytoplankton blooms. Curbing algal growth helped maintain turbidity levels at a low level inside the pond (i.e. 3.7 ± 0.3 NTU, mean ± S.E.), allowing behavioral observations with cameras.

2.2. Feeding protocol

The trial was repeated three times in the same pond from July to October 2021 with unique groups of shrimp for each trial. Trials comprised 6 days of observation, following the initial acclimation period of 7 days. Three stereo cameras (ZED 2 from Stereolabs Inc., USA) mounted on tripods 45 cm above the pond bottom were positioned equidistant from each other inside waterproof Plexiglas casings (Fig. 1), providing a top to bottom view of the pond. Four red underwater lights (wavelength > 600 nm) were provided in conjunction with each camera, secured to the tripod and directed towards the bottom of the pond, in the middle of the field of view to facilitate observations of shrimp (see below). The lights remained on continuously to maintain consistency across all observations. Although it is possible that continuous red light may have an effect on shrimp behavior, this is unlikely as decapod crustaceans lack sensitivity to near-infrared wavelengths (Johnson et al., 2002; Weiss et al., 2006). These lights can therefore be used to enhance tracking results during cloudy days and at night. Cameras were placed inside the pond before the acclimation period began, allowing the animals to become familiar with their presence. Feed was provided through a PVC pipe below either camera 1 or 3 (with camera 2 in the middle, Fig. 1). Feed was dispersed within a narrow spreading radius approximately 1 m in diameter allowing for accurate delimitation of the feeding areas (Fig. 1), and taking less than 10 s to be delivered.

Each morning the position of the feeding area was alternated between cameras 1 and 3. A 20-min observation period was recorded from each of the three cameras simultaneously, comprising 10 min before and 10 min after feeding. Cameras were connected to computers by a USB 3.0 cable and remotely controlled via ZED Explorer (Stereolabs Inc.,

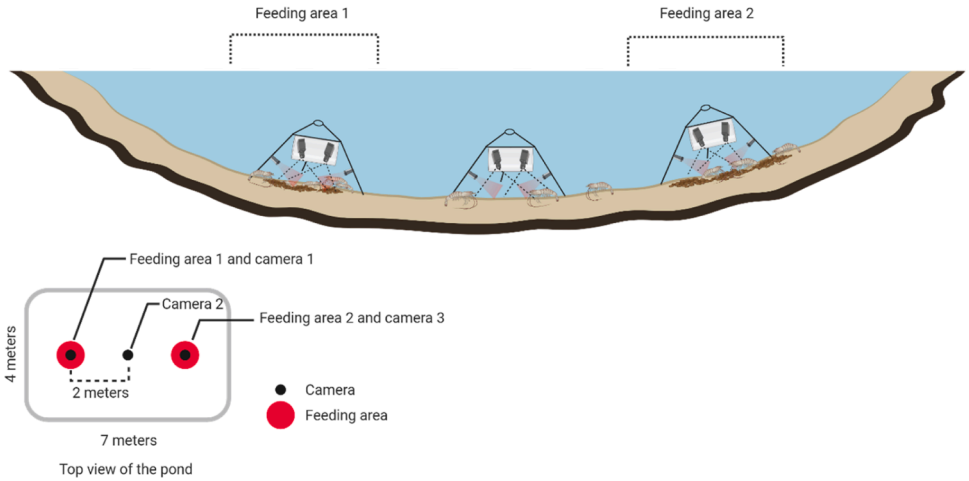

Fig. 1. Side view of the camera and feeding area layout inside the pond, with a diagram of the top view of the pond (lower-left corner). Each observation system comprised a stereo camera (2 lenses) mounted on a tripod with red lights pointing towards the observed portion of the bottom. Created with BioRender.com.

USA). Every day, three feeding times (i.e. 'Times of day'; 07:30, 12:00, 19:00) were filmed on all cameras. These three meals were chosen for filming due to their proximity to sunrise, midday, and sunset where changes in shrimp behavior were most expected. For each recording, 5 s of footage was extracted 10 min before feeding, 1 min after the beginning of feed dispersal (considered as 'during feeding' in later analyses) and 10 min after feed distribution to calculate behavioral metrics (Table 1). The first frame of every 5 s of footage was also extracted to allow for measurement of shrimp length and orientation using ImageJ (Table 1).

Table 1
Details of the metrics obtained from the footage extracts, adapted from Viscido et al. (2004) and Somerton et al. (2017).

Metric	Description
Density of individuals	$D = N/A$ Where D is the local density of individuals (ind.m^{-2}), N the number of detected individuals and A the pond bottom area covered by the camera's field of view.
Individual speed	$S_i = \sqrt{V_{x,i}^2 + V_{y,i}^2}$ Where S_i is the mean velocity of individual i (cm.s^{-1}), and $V_{x,i}$, $V_{y,i}$ the individual velocities in each dimension (as the difference in coordinates between two consecutive frames of footage divided by the elapsed time).
Individual size	The average size (cm) of all observed individuals on a randomly selected frame for each 5 s footage.
Nearest neighbor distances (NND)	$NND_i = \min(d_{i,1}, \quad d_{i,2}, \ldots, \quad d_{i,n})$ Where $d_{i,k}$ is the distance (cm) between the ith individual and individual number k, and n the number of individuals available in the frame at a given time.
Angular deviation with the direction of the feeding area	The mean of angular deviation (°) between the average shrimp heading direction and the direction of the feeding area on a randomly selected frame for each 5 s sample. It is expressed in degrees from the direction of the fed area set at 0° and is between 0 and 180°. The average shrimp heading direction (α) is defined as: $\alpha = \text{atan2} \sum_{i=1}^{n} \sin(\alpha_i)$ Where α_i is the heading direction of shrimp number i.
Group speed	$S_g = \sqrt{U_x{}^2 + U_y{}^2}$ Where S_g is the group speed (cm.s^{-1}), and U_x and U_y the group velocities for each axis (defined as the difference in the mean positions of all detected individuals between two consecutive frames divided by the elapsed time).
Polarity	$\theta^* = 1 - \sum_{i=1}^{n} \beta_i/(90 * n)$ Where θ^* represents the average polarity (between 0 and 1, no unit), β_i the angular deviation (°) between the heading direction of shrimp number i and the average shrimp heading direction of the group (α) and n the number of detected shrimp.

2.3. Camera calibration

Intrinsic parameters of the cameras were calibrated using the camera calibration toolbox on OpenCV for Python 3, taking into account distortion effects from the various media the light travelled through (i.e. water, plastic and air) before reaching the lenses. For each camera, lens and resolution, calibration was performed on 50 images from a chessboard pattern taken underwater at different angles. A 15 cm graduated arrow on the pond bottom within the camera field of view was used to calibrate distances and image orientation.

Recorded footage was analyzed for shrimp identification and tracking at 5 FPS (frames per second) using a customized software based on the image instantiation algorithm YOLACT (Bolya et al., 2019), optimized for high density object segmentation and overlapping of objects. This deep neural network was previously trained with a comprehensive and manually labelled dataset. Initial training was performed on a total of 330 frames from all three cameras in various lighting conditions (i.e. different time of day, weather and turbidity conditions), with varying numbers of shrimp. Training consisted of manually drawing polygons around the shrimp using the DarkLabel utility program. Animal detection with YOLACT resulted in two sets of coordinates for each detected individual in Microsoft Excel, as a single detection corresponds to a bounding box on the frame (in this case, a rectangle, sets of coordinates are given for two opposite corners of the bounding box). The center position for the shrimp body was calculated as follows (Hatton-Jones et al., 2021):

$$Central\ body\ position(x, \quad y) = \quad (x_{max} + x_{min})/2, \qquad (y_{max} + y_{min})/2$$

Trajectory generation (i.e. for each frame, the association of the detected animals to the tracked individuals; Panadeiro et al., 2021) was performed manually using Microsoft Excel, and missing coordinates in the tracking results were obtained using Microsoft Excel's fill option for linear series. Visual checks of the tracking outputs on all the videos were performed to ensure accuracy of the results. When water conditions were too challenging or the number of shrimp too high for the software to reliably identify and track the animals (i.e. approximately 25 % of the videos), shrimp coordinates were manually obtained through the animal tracking software EthoVision XT V14s (Noldus et al., 2001) using the manual tracking feature of the program. The chosen system of coordinates was the one provided by EthoVision, where x = 0 and y = 0 corresponds to the image center, and coordinates increase from left to right and from bottom to top. Centimeters were chosen as the common

unit for all coordinates. ImageJ software (Schneider et al., 2012) was used to measure observed shrimp length and orientation. Different computers were used to analyse videos with YOLACT (CPU: Intel Xeon CPU E5–2630 @ 2.20 GHz (20 Cores), Memory: 32 GB Ram, GPU: Nvidia GeForce GTX TITAN 12 GB RAM with 3072 CUDA cores), EthoVision and ImageJ (Intel Core i7–10750H @ 2.6 GHz (1 core), Memory: 8 GB Ram, GPU: Nvidia GeForce GTX 1660) which affected processing time but not the accuracy of results provided.

2.4. Statistical analysis

All statistics were performed using R statistical software v. 4.0.5 (R Core Team, 2023). The effects of camera location (i.e. fed, camera 2 (close to the feed) and unfed (far from the feed)) and feed distribution (before, during and after) were assessed on behavioral metrics calculated as defined by Viscido et al. (2004) and Somerton et al. (2017) (Table 1). Multivariate generalized mixed-effect models (GLMM) were built for each behavioral metric with feed provision, camera location and their interaction as fixed factors and camera ID nested within trial ID as a random factor using the R package 'lme4' (Zuur et al., 2009; Bates et al., 2022). Trial ID was included as a random factor to account for any variation in physical parameters between trials (e.g. temperature, dawn/dusk times). Although underwater visibility was controlled as well as possible, observation sessions sometimes resulted in visually challenging recordings, especially at night where shrimp could still be spotted but accurate estimates of metrics related to their movements and size could not be obtained. For some observations, only a few individuals were present below the cameras, resulting in an observed number of individuals of 0 or 1, but with no associated individual and/or group behavioral metrics. Consequently, the density of individuals could be observed in a wider range of conditions than the other metrics. Therefore, Time of day (i.e. 'Morning' 07:30, 'Noon' 12:00 and 'Evening' 19:00) and its interaction with the fixed factors mentioned above was included as a fixed factor in models related to the density of individuals (GLMM). Where significant effects were found, post-hoc comparisons between treatments were conducted using the R package 'multcomp' (Hothorn et al., 2021) for main effects and 'lsmeans' for interactions (Lenth, 2018). Density of individuals, angular deviation with the direction of the feeding area and polarity data followed negative binomial distributions. Individual and group speed as well as shrimp size data followed Gamma distributions.

3. Results

A significant effect of feed provision was found on individual speed (Table 2), with individuals moving faster during and after feed dispersal than before (Fig. 2a). However, no effects of camera location and its interaction with feed provision were found on individual speed (Table 2). The size of shrimp was influenced by feed provision, camera location and their interaction (Table 2). Observed individuals appearing beneath camera 2 were larger after feed provision than before (Fig. 2b).

Nearest neighbor distances (NND) were affected by feed provision, camera location and their interaction (Table 2). Individuals beneath the fed camera moved closer to each other during and after feed provision compared to before (Fig. 3a). No differences in NND were observed between camera locations before feed provision (Fig. 3a). A significant effect of camera location was also found on shrimp angular deviation from the direction of the feeding area (Table 2) with individuals below camera 2 showing an orientation angled more towards the feeding area than individuals located under the unfed camera (Fig. 3b).

Camera location, feed provision and their interaction had a significant effect on group polarity i.e. the average alignment in heading direction of individuals relative to that of the group (Table 2; Fig. 4). At each time relative to feed provision, there were no differences in polarity between camera locations. Underneath both camera 2 and the unfed camera, polarity did not change with time relative to feed provision, however, polarity significantly decreased under the fed camera from before feeding to after feeding (Fig. 4).

Table 2
GLMM of the effects of feed provision, camera location and their interaction on key behavioral metrics and density of individuals for *L. vannamei*. Presented with associated χ^2 and p-values, with statistically significant results represented in bold.

Metric	Feed provision		Camera location		Interaction	
	χ^2 (2)	p-value	χ^2 (2)	p-value	χ^2 (4)	p-value
Individual speed ($cm.s^{-1}$)	23.06	**< 0.001**	1.61	0.446	4.54	0.338
Size (cm)	7.93	**0.019**	6.41	**0.041**	9.72	**0.046**
Nearest Neighbor Distances (NND) (cm)	18.29	**< 0.001**	32.21	**< 0.001**	52.73	**< 0.001**
Angular deviation from the direction of the feeding area (°)	0.16	0.924	4.22	**0.040**	0.67	0.715
Group speed ($cm.s^{-1}$)	15.74	**< 0.001**	1.63	0.441	5.17	0.270
Polarity	2.94	0.230	8.49	**0.014**	15.58	**0.004**
Density of individuals ($ind.m^{-2}$)	7.47	**0.024**	104.45	**< 0.001**	90.37	**< 0.001**

The observed density of individuals below the cameras was affected by the time relative to feed provision, camera location and their interaction (Table 2; Fig. 5a). Time of day was included in models related to density of individuals, and had a significant effect (χ^2 (2) = 25.618, $p < 0.001$; Fig. 5b). The number of shrimp under the fed camera increased during and after feeding compared to pre-feeding (Fig. 5a) and there were more individuals under the fed camera compared to the other cameras during and after feed dispersal (Fig. 5a). There were no differences in shrimp density below camera 2 between before, during and after feeding (Fig. 5a). However, there were less individuals below the unfed camera after feeding compared to before and during feeding (Fig. 5a), and there were less observed individuals below the unfed camera after feeding compared to the others (Fig. 5a). There were also less shrimp observed in total in the evening than at noon and in the morning (Fig. 5b).

4. Discussion

In the present study, higher activity occurred during and after feed provision compared to before, with the average speed of individuals increasing significantly. This is in line with previous scuba observations in shrimp aquaculture ponds (McNeil, 2001), where fast movements oriented towards feed occurred immediately after feed provision when it fell within 10 m of the animals. The increased speed in the present study did not depend on camera location, suggesting shrimp were affected across the whole pond. Previous laboratory research found that feed provision induced substrate exploration, with *L. vannamei* sampling the bottom more after feed introduction (Pontes and Arruda, 2005). The area of influence around shrimp feeding stations clearly goes beyond that captured within laboratory studies and we can hypothesize that it is likely to go beyond the size of the pond used here. As seen in Fig. 1, the fed and unfed camera were 4 m apart, and yet the increased speed was not affected by camera location. As the pond was only 7 m in length, feed provision may induce changes in shrimp activity at greater distances, which further research within larger commercial ponds is needed to confirm.

A previous laboratory study on *L. vannamei* found that dominant individuals arrive first to the feeding area and then spend time exploring, whereas subordinates spend more time within the feeding area and less time exploring (Bardera et al., 2021). In the present study,

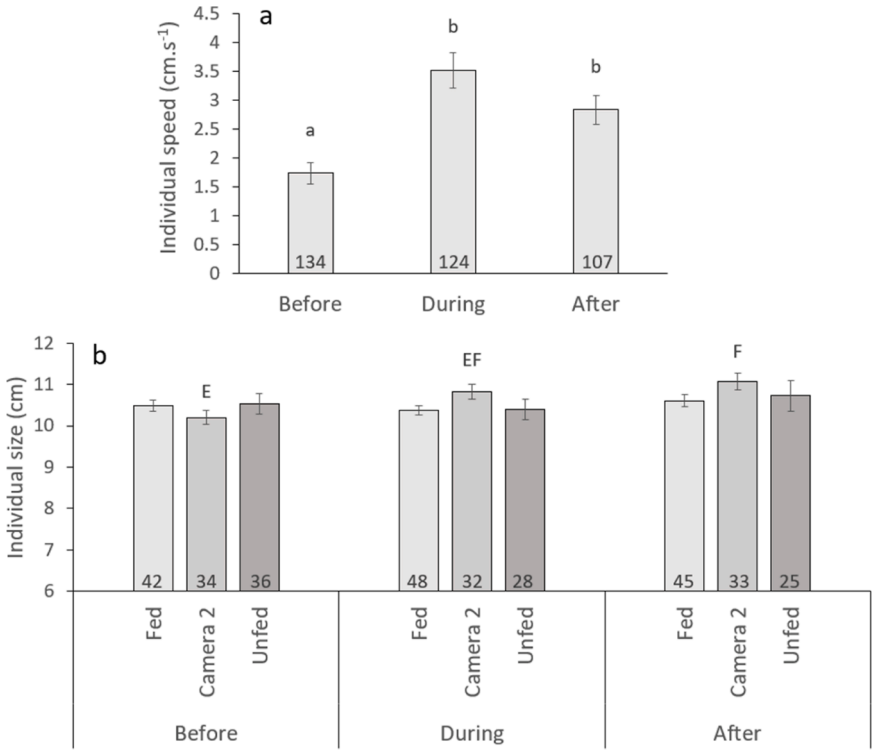

Fig. 2. (a) Individual speeds (cm s^{-1}) of shrimp observed under the cameras against time relative to feed provision. (b) Size (cm) of shrimp observed under the cameras relative to both feed provision and camera location (b). Results are means ± S.E., numbers of observations are indicated inside the bars. For panel (a) significant differences ($p < 0.05$) in individual speeds are indicated by lowercase letters and in panel (b) significant differences ($p < 0.05$) in individual size between feed provision within the same location are indicated by uppercase letters, where bars sharing a letter are not statistically different.

no variation in shrimp size below the fed camera was observed in relation to feed provision but larger shrimp were observed under the camera located between the fed and unfed areas 10 min after feed provision, which may align with laboratory observations. In commercial conditions, larger individuals were first to arrive to feeding trays (McNeil, 2001), remaining on them for 15–20 min but information on dominance hierarchy formation in penaeid shrimp aquaculture ponds is lacking. In the present study, it is possible that low size variation at stocking minimized size gradients between fed and unfed areas. In commercial grow-out ponds, especially several weeks after stocking, size variation can be large (e.g. 1.18 g in mass difference; Reis et al., 2020) and size variation across different pond locations may become more obvious.

A gradient in NND was observed shortly after feed provision, with shrimp closer to each other when inside the feeding area. Shrimp were more oriented towards the feeding area when under the middle camera (camera 2) compared to individuals in the unfed area, however shrimp close to the feeding area were not more aligned with each other than those far from it. Polarity was defined as the average alignment in heading direction of individuals relative to that of the group, taking values ranging from 0 (completely disorganized) to 1 (perfectly aligned). Individuals within the feeding area 10 min after feeding were less polarized than those in the same area before feed was provided. These observations combined with average individual speed and NND, suggest that feed provision induced large scale shrimp movements, with individuals moving faster across the whole pond but in a more disorganized way once within the feeding area. Maximum polarity values (0.52 ± 0.05) were seen underneath the middle camera during feed provision but did not appear indicative of tightly organized groups. Studies on polarity in fish have found values close to 1 for highly organized schools, and values between 0.4 and 0.8 within small groups of giant danios (*Danio aequipinnatus*) or vermilion snapper (*Rhomboplites aurorubens*) (Viscido et al., 2004; Somerton et al., 2017). Previous observations in aquaculture ponds (McNeil, 2001), reported large schools of shrimp forming at sunrise, with a strong shoaling tendency remaining throughout the day. Formation of shoals within aquaculture ponds will likely affect the way shrimp interact with feeding stations in a pond environment, and therefore is an important behavior to understand in the context of feeding efficiencies. The experimental pond in the present study may have been too small to observe these behavioral patterns even though density was representative of commercial Ecuadorian ponds (i.e. 21 ind.m^{-2}, Boyd et al., 2021). The limited pond size reduced the number of individuals stocked, potentially preventing shrimp from gathering in large formations. Whether or not shrimp regularly form large shoals in commercial ponds warrants further investigation.

Density of individuals depended on feed provision, camera location and time of day. During feed provision and for the following 10 min, density was highest under the camera in the fed area indicating an immediate attraction effect. Previous studies using PAM in the laboratory and aquaculture ponds, also reported intense feeding shortly after feed provision, declining over a 25 min period (Smith and Shahriar, 2013; Smith and Tabrett, 2013). Hamilton et al. (2023) observed that acoustic activity occurred immediately after feed provision and lasted up to 10 min, suggesting shrimp quickly reached a state of satiation after feeding. Visual observations in laboratory conditions also found a higher feeding activity 30 min after feed was offered (Nunes et al., 1996; Pontes and Arruda, 2005). The significant interaction effect of feed provision and camera location on density indicates a gradient in shrimp density established over time once feed was introduced. The highest density was in the feeding area and the lowest under the unfed camera on the other edge of the pond. This gradient did not last until the next feed with no interaction between camera location and time of day, potentially indicating a lack of anticipatory behavior.

Under all cameras the number of individuals was lowest in the evening. Morning observations (07:30) occurred between 1 h 10 min and

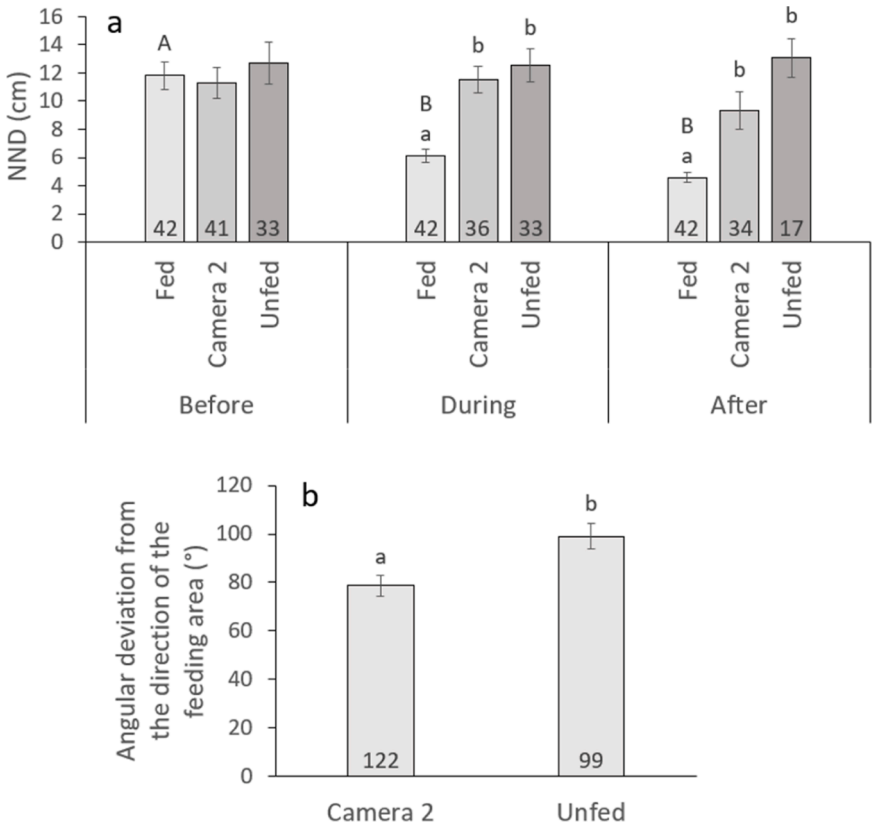

Fig. 3. (a) Nearest Neighbour Distances (NND) of shrimp observed under the cameras against time relative to feed provision and camera location. (b) Angular deviation of shrimp observed under the cameras from the direction of the feeding area against camera location. Results are means ± S.E., numbers of observations are indicated inside the bars. For panel (a), significant differences in NND between times around feed provision events at the same location are indicated by uppercase letters and significant differences at the same time around feed provision but at different locations are indicated by lowercase letters, where bars sharing a letter are not statistically different. For panel (b), significant differences in angular deviation with the direction of the feeding area are indicated by lowercase letters, where bars sharing a letter are not statistically different.

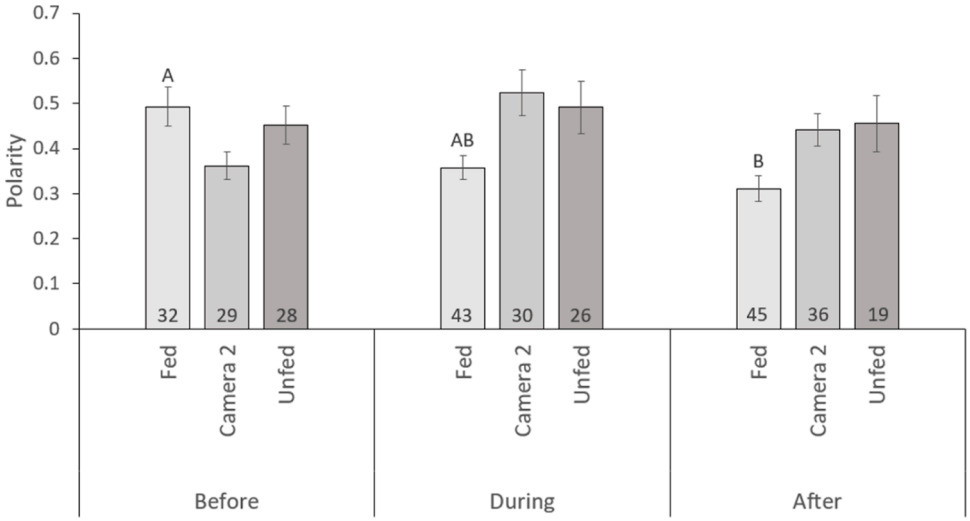

Fig. 4. Differences in average polarity of shrimp observed under the cameras against time relative to feed provision and location. Results are means ± S.E., numbers of observations are indicated inside the bars. Significant differences between times around feed provision at the same location are indicated by uppercase letters where bars sharing a letter are not statistically different.

1 h 41 min after sunrise, and evening observations (19:00) between 14 min before and 58 min after sunset. Therefore, most evening observations occurred at night, but morning observations were all during daylight hours. Previous studies under laboratory conditions reported diel patterns of activity in penaeid shrimp (Pontes and Arruda, 2005; Pontes et al., 2006; De Lima et al., 2009). Pontes et al. (2006) observed that inactivity was predominant in the light phase for *L. vannamei*, but food searching occurred both during day and night with the most intense peak 7 h after lights were turned on. This corresponds to ~ 13:00 in the present study. Similarly, De Lima et al. (2009) reported greater feed

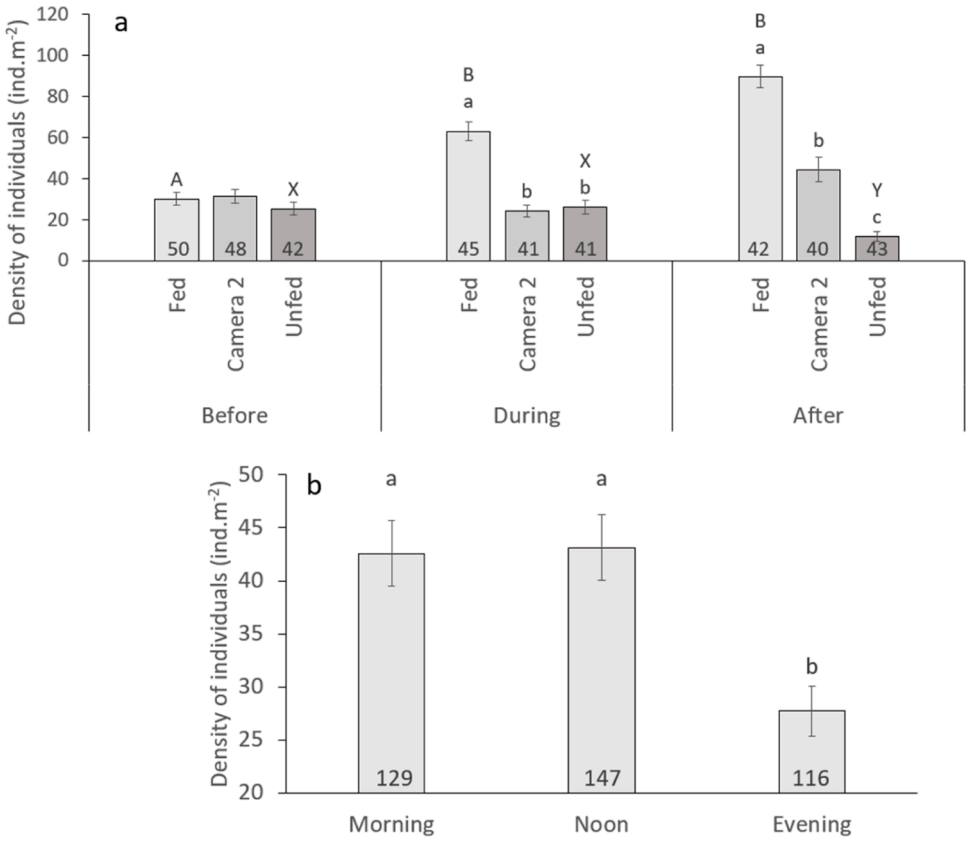

Fig. 5. (a) Shrimp density (ind.m^{-2}) observed under the cameras against time relative to feed provision and camera location. (b) Shrimp density (ind.m^{-2}) observed under all cameras against time of day. Results are means ± S.E., numbers of observations are indicated inside the bars. For panel (a), significant differences ($p < 0.05$) in density between times around feed provision at the same location are indicated by uppercase letters, significant differences ($p < 0.05$) in density at the same time around feed provision but at different locations are indicated by lowercase letters, where bars sharing a letter are not statistically different. For panel (b), significant differences are indicated by lowercase letters, where bars sharing a letter are not statistically different.

ingestion between 12:00 and 14:00 for *L. vannamei*. Observed densities in the morning and at noon below all cameras was more than twice the theoretical stocking density of 20 ind.m^{-2}, suggesting an uneven distribution during daytime. A previous study on the gut contents of *Penaeus subtilis* in aquaculture ponds reported continuous feeding during both day and night, with a peak observed soon after dusk, even when no pellets were provided (Nunes et al., 1996). As shrimp are scavenging opportunistic feeders (Tacon et al., 2013), it is possible that at night when provision of artificial feed ceases, shrimp focus more on natural food sources thereby scattering throughout the pond.

Overall, this study provided an insight into how shrimp organize themselves in ponds, to help answer the key questions of when and where feed should be provided. In commercial aquaculture settings, use of PAM to monitor shrimp feeding is preferred since sound is not affected by underwater visibility (Reis et al., 2022). However, the present study demonstrates the potential for computer vision to further our understanding of shrimp behavior. Similar approaches are used to automate assessment of fish feeding in aquaculture cages, tanks and ponds using neural networks on video frames (e.g. Måløy et al., 2019; Zhou et al., 2019; Ubina et al., 2021). In the present study, observations were made in an experimental pond, under relatively controlled conditions, with animals well matched in size. In shrimp aquaculture, a wide variety of production systems and genetic lines exist, which could potentially affect behavior. The average *L. vannamei* pond in Vietnam is 0.33 ha in surface area, stocked at 55 ind.m^{-2}, whereas in Ecuador ponds are often 6.59 ha in size and stocked at 21 ind.m^{-2} (Boyd et al., 2021). The present study focused on *L. vannamei*, and although it represents more than 90 % of global penaeid aquaculture, the giant tiger prawn *Penaeus monodon* is another important species (FIGIS, 2023) whose behavior is still to be fully explored.

5. Conclusion

The present study demonstrated the potential of remote video observations to provide a better understanding of shrimp behavior, highlighting the influence of time of day, camera location and feed provision on penaeid shrimp (*L. vannamei*) behavior in an experimental aquaculture pond. Combination of computer vision techniques to observe behavioral detail, with PAM monitoring of shrimp feeding through hydrophones could result in the adoption of smarter feeding practices in penaeid aquaculture, relevant to the behavior of the animal. In the present study, shrimp speed increased and more individuals were present inside the feeding area after feed provision. The development of an automated assessment of shrimp feeding may therefore be achievable through computer vision, based on the observed number of individuals and their velocity. More generally, computer vision could enhance welfare monitoring through the early detection of unusual behaviors indicating a stress response, as already observed in laboratory conditions (Zhang et al., 2006). Future work should focus on trialing similar approaches under commercial conditions, across a variety of production models and species. Setting cameras in association with sonar-based systems at different pond locations could help farmers better position feeders by providing a more complete picture of areas where shrimp congregate, as well as their preferred passage points in relation to depth and distance from pond banks.

CRediT authorship contribution statement

Jean-Benoît Darodes de Tailly: Writing – original draft, Methodology, Investigation, Formal analysis, Conceptualization. **Ignacio Martinez Alpiste**: Writing – review & editing, Investigation, Formal analysis, Conceptualization. **Matthew A.G. Owen**: Writing – review & editing, Conceptualization. **Jonas Keitel**: Writing – review & editing, Conceptualization. **Jose M. Alcaraz-Calero**: Writing – review & editing, Conceptualization. **Katherine A. Sloman**: Writing – review & editing, Supervision, Funding acquisition, Conceptualization. **Mhairi E. Alexander**: Writing – review & editing, Supervision, Formal analysis, Conceptualization.

Declaration of Competing Interest

The authors declare that they have no known competing financial interests or personal relationships that could have appeared to influence the work reported in this paper

Acknowledgments

The authors would like to thank Skretting AI for providing funding and materials. The authors also thank Skretting's research center in Zhuhai for conducting the trials and particularly Lionel Liu and Lanhong Li for making this study possible during the Covid pandemic.

References

Bardera, G., Owen, M.A.G., Façanha, F.N., Alcaraz-Calero, J.M., Alexander, M.E., Sloman, K.A., 2021. The influence of density and dominance on Pacific white shrimp (*Litopenaeus vannamei*) feeding behaviour. Aquaculture 531, 735949.

Bates, D., Maechler, M., Bolker, B., & Walker, S. (2022). lme4: Linear Mixed-Effects Models using 'Eigen' and S4 (R package version 1.1-27). Available from URL: ⟨http://CRAN.R-project.org/package=lme4⟩.

Bolya, D., Zhou, C., Xiao, F., & Lee, Y.J. (2019). Yolact: Real-time instance segmentation. In *Proceedings of the IEEE/CVF International Conference on Computer Vision* (pp. 9157-9166).

Boyd, C.E., Davis, R.P., McNevin, A.A., 2021. Comparison of resource use for farmed shrimp in Ecuador, India, Indonesia, Thailand, and Vietnam. Aquac., Fish. Fish. 1 (1), 3–15.

Cao, S., Zhao, D., Liu, X., Sun, Y., 2020. Real-time robust detector for underwater live crabs based on deep learning. Comput. Electron. Agric. 172, 105339.

Darodes de Tailly, J.B., Keitel, J., Owen, M.A., Alcaraz-Calero, J.M., Alexander, M.E., Sloman, K.A., 2021. Monitoring methods of feeding behaviour to answer key questions in penaeid shrimp feeding. Rev. Aquac. 13, 1828–1843.

De Lima, P.P., Pontes, C.S., Arruda, M. de F., 2009. Activity pattern of the marine shrimp *Litopenaeus vannamei* (Boone 1931) in the laboratory as a function of different feeding frequencies. Aquac. Res. 41, 53–60.

Engle, C.R., McNevin, A., Racine, P., Boyd, C.E., Paungkaew, D., Viriyatum, R., Tinh, H. Q., Minh, H.N., 2017. Economics of Sustainable Intensification of Aquaculture: Evidence from Shrimp Farms in Vietnam and Thailand. J. World Aquac. Soc. 48, 227–239.

FIGIS. (2023). FAO Statistics. Global aquaculture production 1950–2019. Available from URL: ⟨http://www.fao.org/fishery/statistics/global-aquaculture-production/query/en⟩.

Hamilton, S., Costa Filho, F., Silva, J.F., Duarte-Neto, P.J., Soares, R., Peixoto, S., 2023. The loud crowd: Interactions between stocking density and acoustic feeding activity of different size classes of *Litopenaeus vannamei*. Aquaculture 563, 738904.

Hatton-Jones, K.M., Christie, C., Griffith, T.A., Smith, A.G., Naghipour, S., Robertson, K., Russell, J.S., Peart, J.N., Headrick, J.P., Cox, A.J., du Toit, E.F., 2021. A YOLO based software for automated detection and analysis of rodent behaviour in the open field arena. Comput. Biol. Med. 134, 104474.

Hothorn, T., Bretz, F., Westfall, P., Heiberger, R.M., Schuetzenmeister, A., & Scheibe, S. (2021). multcomp: Simultaneous inference in general parametric models (R package version 1.4-17). Available from URL: ⟨https://cran.r-project.org/web/packages/multcomp/index.html⟩.

Israeli, D., Kimmel, E., 1996. Monitoring the behavior of hypoxia-stressed *Carassius auratus* using computer vision. Aquac. Eng. 15, 423–440.

Johnson, M.L., Gaten, E., Shelton, P.M.J., 2002. Spectral sensitivities of five marine decapod crustaceans and a review of spectral sensitivity variation in relation to habitat. J. Mar. Biol. Assoc. U. Kingd. 82, 835–842.

Kadri, S., Huntingford, F.A., Metcalfe, N.B., Thorpe, J.E., 1996. Social interactions and the distribution of food among one-sea-winter Atlantic salmon (*Salmo salar*) in a sea-cage. Aquaculture 139, 1–10.

Lai, P.C., Lin, H.Y., Lin, J.Y., Hsu, H.C., Chu, Y.N., Liou, C.H., Kuo, Y.F., 2022. Automatic measuring shrimp body length using CNN and an underwater imaging system. Biosyst. Eng. 221, 224–235.

Lenth, R. (2018). lsmeans: Least-squares means (R Package Version 2.30-0). Available from URL: ⟨http://cran.r-project.org/package=lsmeans⟩.

Li, X., Shang, M., Hao, J., Yang, Z., 2016. Accelerating fish detection and recognition by sharing CNNs with objectness learning. In *OCEANS 2016 – Shanghai*. IEEE, pp. 1–5.

Lin, Y.-C., Chen, J.-C., 2001. Acute toxicity of ammonia on *Litopenaeus vannamei* Boone juveniles at different salinity levels. J. Exp. Mar. Biol. Ecol. 259, 109–119.

Lin, Y.-C., Chen, J.-C., 2003. Acute toxicity of nitrite on *Litopenaeus vannamei* (Boone) juveniles at different salinity levels. Aquaculture 224, 193–201.

Mahmood, A., Bennamoun, M., An, S., Sohel, F., Boussaid, F., Hovey, R., Kendrick, G., 2020. Automatic detection of Western rock lobster using synthetic data. ICES J. Mar. Sci. 77, 1308–1317.

Måløy, H., Aamodt, A., Misimi, E., 2019. A spatio-temporal recurrent network for salmon feeding action recognition from underwater videos in aquaculture. Comput. Electron. Agric. 167, 105087.

Martinez-Alpiste, I., de Tailly, J.B., Alcaraz-Calero, J.M., Sloman, K.A., Alexander, M.E., Wang, Q., 2024. Machine learning-based understanding of aquatic animal behaviour in high-turbidity waters. Expert Syst. Appl. 255, 124804.

Martins, C.I., Galhardo, L., Noble, C., Damsgård, B., Spedicato, M.T., Zupa, W., et al., 2012. Behavioural indicators of welfare in farmed fish. Fish. Physiol. Biochem. 38, 17–41.

McNeil, R. (2001). Shrimp Behavior 101. Shrimp News International. Available from URL: ⟨https://www.shrimpnews.com/FreeReportsFolder/PondEcologyFolder/ShrimpBehaviorMcNeil.html⟩.

Noldus, L.P.J.J., Spink, A.J., Tegelenbosch, R.A.J., 2001. EthoVision: a versatile video tracking system for automation of behavioral experiments. Behav. Res. Methods, Instrum., Comput. 33, 398–414.

Nunes, A.J.P., Goddard, S., Gesteira, T.G.V., 1996. Feeding activity patterns of the Southern brown shrimp *Penaeus subtilis* under semi-intensive culture in NE Brazil. Aquaculture 144, 371–386.

Panadeiro, V., Rodriguez, A., Henry, J., Wlodkowic, D., Andersson, M., 2021. A review of 28 free animal-tracking software applications: current features and limitations. Lab Anim. 50, 246–254.

Pautsina, A., Císař, P., Štys, D., Terjesen, B.F., Espmark, Å.M.O., 2015. Infrared reflection system for indoor 3D tracking of fish. Aquac. Eng. 69, 7–17.

Pedersen, M., Bruslund Haurum, J., Gade, R., & Moeslund, T.B. (2019). Detection of marine animals in a new underwater dataset with varying visibility. In *Proceedings of the IEEE Conference on Computer Vision and Pattern Recognition Workshops* (pp. 18–26).

Pontes, C.S., Arruda, M. de F., 2005. Comportamento de *Litopenaeus vannamei* (Boone) (Crustacea, Decapoda, Penaeidae) em função da oferta do alimento artificial nas fases clara e escura do período de 24 horas. Rev. Bras. De. Zool. 22, 648–652.

Pontes, C.S., Arruda, M.F., Menezes, A.A., Lima, P.P., 2006. Daily activity pattern of the marine shrimp *Litopenaeus vannamei* (Boone 1931) juveniles under laboratory conditions. Aquac. Res. 37, 1001–1006.

R Core Team. (2023). R: A language and environment for statistical computing. R Foundation for Statistical Computing, Vienna, Austria. Available from URL: ⟨https://www.R-project.org/⟩.

Redmon, J., Divvala, S., Girshick, R., & Farhadi, A. (2016). You Only Look Once: Unified, real-time object detection. In 2016 *IEEE Conference on Computer Vision and Pattern Recognition (CVPR)*, (pp. 779–788).

Reis, J., Novriadi, R., Swanepoel, A., Jingping, G., Rhodes, M., Davis, D.A., 2020. Optimizing feed automation: improving timer-feeders and on-demand systems in semi-intensive pond culture of shrimp *Litopenaeus vannamei*. Aquaculture 519, 734759.

Reis, J., Peixoto, S., Soares, R., Rhodes, M., Ching, C., Davis, D.A., 2022. Passive acoustic monitoring as a tool to assess feed response and growth of shrimp in ponds and research systems. Aquaculture 546, 737326.

Sadoul, B., Mengues, P.E., Friggens, N.C., Prunet, P., Colson, V., 2014. A new method for measuring group behaviors of fish shoals from recorded videos taken in near aquaculture conditions. Aquaculture 430, 179–187.

Sanchez, D.R., Fox, J.M., Lawrence, A.L., Castille, F.L., Dunsford, B., 2005. A methodology for the evaluation of dietary feeding stimulants for the Pacific white shrimp, *Litopenaeus vannamei*. J. World Aquac. Soc. 36, 14–23.

Schneider, C.A., Rasband, W.S., Eliceiri, K.W., 2012. NIH Image to ImageJ: 25 years of image analysis. Nat. Methods 9, 671–675.

Silva, P.F., Medeiros, M.S., Silva, H.P.A., Arruda, M.F., 2012. A study of feeding in the shrimp *Farfantepenaeus subtilis* indicates the value of species-level behavioral data for optimizing culture management. Mar. Freshw. Behav. Physiol. 45, 121–134.

Smith, D.V., Shahriar, M.S., 2013. A context-aware sound classifier applied to prawn feed monitoring and energy disaggregation. Knowl. -Based Syst. 52, 21–31.

Smith, D.V., Tabrett, S., 2013. The use of passive acoustics to measure feed consumption by *Penaeus monodon* (giant tiger prawn) in cultured systems. Aquac. Eng. 57, 38–47.

Somerton, D.A., Williams, K., Campbell, M.D., 2017. Quantifying the behavior of fish in response to a moving camera vehicle by using benthic stereo cameras and target tracking. Fish. Bull. 115, 343–354.

Tacon, A.G.J., Jory, D., Nunes, A., 2013. Shrimp feed management: issues and perspectives. In: Hasan, M.R., New, M.B. (Eds.), On-farm Feeding and Feed Management in Aquaculture. FAO Fisheries and Aquaculture Technical Paper, pp. 481–488.

Ubina, N., Cheng, S.C., Chang, C.C., Chen, H.Y., 2021. Evaluating fish feeding intensity in aquaculture with convolutional neural networks. Aquac. Eng. 94, 102178.

Ullman, C., Rhodes, M., Hanson, T., Cline, D., Davis, D.A., 2017. A new paradigm for managing shrimp feeding. World Aquac. 2017, 31.

Viscido, S., Parrish, J., Grünbaum, D., 2004. Individual behavior and emergent properties of fish schools: a comparison of observation and theory. Mar. Ecol. Prog. Ser. 273, 239–249.

Weiss, H.M., Lozano-Álvarez, E., Briones-Fourzán, P., Negrete-Soto, F., 2006. Using red light with fixed-site video cameras to study the behavior of the spiny lobster, *Panulirus argus*, and associated animals at night and inside their shelters. Mar. Technol. Soc. J. 40, 86–95.

Xu, J., Liu, Y., Cui, S., Miao, X., 2006. Behavioral responses of tilapia (*Oreochromis niloticus*) to acute fluctuations in dissolved oxygen levels as monitored by computer vision. Aquac. Eng. 35, 207–217.

Yang, L., Liu, Y., Yu, H., Fang, X., Song, L., Li, D., Chen, Y., 2021. Computer vision models in intelligent aquaculture with emphasis on fish detection and behavior analysis: A review. Arch. Comput. Methods Eng. 28, 2785–2816.

Zhang, P., Zhang, X., Li, J., Huang, G., 2006. The effects of body weight, temperature, salinity, pH, light intensity and feeding condition on lethal DO levels of whiteleg shrimp, *Litopenaeus vannamei* (Boone, 1931). Aquaculture 256, 579–587.

Zhou, C., Zhang, B., Lin, K., Xu, D., Chen, C., Yang, X., Sun, C., 2017. Near-infrared imaging to quantify the feeding behavior of fish in aquaculture. Comput. Electron. Agric. 135, 233–241.

Zhou, C., Lin, K., Xu, D., Chen, L., Guo, Q., Sun, C., Yang, X., 2018. Near infrared computer vision and neuro-fuzzy model-based feeding decision system for fish in aquaculture. Comput. Electron. Agric. 146, 114–124.

Zhou, C., Xu, D., Chen, L., Zhang, S., Sun, C., Yang, X., Wang, Y., 2019. Evaluation of fish feeding intensity in aquaculture using a convolutional neural network and machine vision. Aquaculture 507, 457–465.

Zuur, A.F., Ieno, E.N., Walker, N.J., Saveliev, A.A., Smith, G.M., 2009. Mixed Effects Models and Extensions in Ecology with R. Springer, New York.